SPE 89429

Theoretical Development of the Brooks-Corey Capillary Pressure Model from Fractal Modeling of Porous Media

Kewen Li, SPE, Stanford University

This paper was prepared for presentation at the 2004 SPE/DOE Fourteenth Symposium on Improved Oil Recovery held in Tulsa, Oklahoma, U.S.A., 17–21 April 2004.

Abstract

The capillary pressure model proposed empirically by Brooks and Corey has been used widely for several decades. However it is not clear why the Brooks-Corey capillary pressure model works so well. In this study, it has been found that the empirical Brooks-Corey capillary pressure model can be derived theoretically from fractal modeling of porous media. Also found was the correlation between the pore size distribution index in the Brooks-Corey capillary pressure model and the fractal dimension. The pore size distribution index increases with the decrease in fractal dimension of the porous media. Capillary pressure curves of different types of rock samples were measured using a mercury intrusion technique. The values of pore size distribution index and fractal dimension were calculated. The relationship between the two parameters obtained from the experimental data was consistent with the relationship derived theoretically. This implies that the fractal dimension of porous media may be inferred directly using the Brooks-Corey capillary pressure model instead of the fractal model. The theoretical development in this study demonstrates that the Brooks-Corey capillary pressure model, once considered as empirical, has a solid theoretical base. This may be why the Brooks-Corey capillary pressure model works satisfactorily in many cases.

Introduction

Capillary pressure plays an important role in many recovery processes. It is essential to represent capillary pressure curves properly. The frequently-used model to express a capillary pressure curve mathematically is the Brooks-Corey capillary pressure model[1]. Brooks and Corey[1] conducted analysis for the capillary pressure curves of a large number of consolidated core samples. The capillary pressure curves were measured using a desorption approach. Brooks and Corey[1] found that the relationship between the capillary pressure and the normalized or effective wetting-phase saturation was a straight line on a log-log plot. The mathematical expression of this relationship was known as the Brooks-Corey capillary pressure model later. Residual wetting-phase saturation must be known or assumed to calculate the normalized or effective wetting-phase saturation. In the analysis by Brooks and Corey[1], the residual wetting-phase saturation was chosen such that the data fit as closely as possible to a straight line when plotted on log-log paper.

The Brooks-Corey capillary pressure model works satisfactorily in many cases and has been utilized widely for several decades in petroleum and other industries[2-7]. However it is not clear why the Brooks-Corey capillary pressure model works so well. Note that the capillary pressure model was proposed empirically by Brooks and Corey[1].

Many researchers[8-20] have studied the fractal nature of reservoir rocks and other porous media in the past two decades. It has been found that most natural porous media such as reservoir rock are fractals and can be characterized using a fractal model or a fractal curve which represents the relationship between the number of pores and the radius of pores. Such a fractal curve is a straight line on a log-log plot and the slope of the straight line is referred to as the fractal dimension of the porous media. The magnitude of fractal dimension is a representation of the heterogeneity of the porous medium. The greater the fractal dimension, the greater the heterogeneity of the porous media. Note that the pore size distribution index in the Brooks-Corey capillary pressure model is also a representation of the heterogeneity of porous media. The greater the pore size distribution index, the more homogeneous the porous medium.

Attention has also been paid to the application of fractal modeling of porous media in reservoir engineering. The applications include the development of relative permeability models, capillary pressure models, and the models to predict oil production rate, *etc*. The author reviewed the literature in this area in a previous paper[18]. The review shows that the fractal modeling of porous media is a powerful tool to characterize the heterogeneity of porous media and to study fluid flow mechanisms.

In this study, we conducted a theoretical development based on the fractal geometry to derive the Brooks-Corey capillary pressure model. Capillary pressure curves of Berea, chalk, and reservoir sandstone were measured using a mercury intrusion technique to infer the fractal dimension. The values of fractal dimension were calculated using the fractal model and the Brooks-Corey capillary pressure model respectively and the results were compared.

Methodology

In this section, the Brooks-Corey capillary pressure model is derived theoretically using the results from fractal modeling.

Previously the author[18] obtained a relationship between the derivative of mercury (nonwetting phase) saturation and the capillary pressure using the theory of fractal geometry. The relationship is expressed as follows:

$$\frac{dS_{Hg}}{dP_c} = aP_c^{-(3-D_f)} \tag{1}$$

where a is a constant, S_{Hg} is the mercury (nonwetting phase) saturation, P_c is the capillary pressure, and D_f is the fractal dimension of the porous media.

As pointed out by the author[18], if a three-dimensional pore model, instead of a two-dimensional capillary tube model, were used to calculate the number of pores in porous media, the following equation can be obtained:

$$\frac{dS_{Hg}}{dP_c} = aP_c^{-(4-D_f)} \tag{2}$$

Eq. 2 was also derived by Friesen and Mikula[9] using a different approach. Eq. 2 can be represented as a more general form in terms of the nonwetting phase saturation:

$$\frac{dS_{nw}}{dP_c} = aP_c^{-(4-D_f)} \tag{3}$$

where S_{nw} is the saturation of the nonwetting phase.

Assuming that P_c approaches to p_e when S_{nw} = 0, integrate Eq. 3:

$$\int_0^{1-S_w} dS_{nw} = a\int_{p_e}^{P_c} P_c^{-(4-D_f)}dP_c \tag{4}$$

where S_w is the saturation of the wetting phase and p_e is the entry capillary pressure.

According to Eq. 4, one can obtain:

$$1-S_w = b[P_c^{-(3-D_f)} - p_e^{-(3-D_f)}] \tag{5}$$

where b is another constant. Assuming that P_c approaches infinity when S_{nw} = 1- S_{wr}, one can obtain according to Eq. 5:

$$1-S_{wr} = -bp_e^{-(3-D_f)} \tag{6}$$

where S_{wr} is the residual saturation of the wetting phase.

It is assumed that fractal dimension D_f is less than 3 in deriving Eq. 6 from Eq. 5.

Combining Eqs. 5 and 6:

$$\frac{1-S_w}{1-S_{wr}} = 1-(\frac{P_c}{p_e})^{-(3-D_f)} \tag{7}$$

Reducing Eq. 7, one can obtain:

$$P_c = p_e(S_w^*)^{-\frac{1}{\lambda}} \tag{8}$$

here S_w^* is the normalized saturation of the wetting phase and is expressed as follows:

$$S_w^* = \frac{S_w - S_{wr}}{1-S_{wr}} \tag{9}$$

and $\lambda = 3 - D_f$.

Eq. 8 is the frequently-used Brooks-Corey capillary pressure model proposed empirically by Brooks and Corey[1] in 1964.

One can see from the previous derivation of Eq. 8 that the Brooks-Corey capillary pressure model has a solid theoretical base. This may explain why this model has been found to be suitable for many types of rock, including reservoir and artificial core samples.

The theoretical model showed that the pore size distribution index increases with the decrease in fractal dimension ($\lambda = 3 - D_f$). This is reasonable because porous media with greater heterogeneity have smaller values of pore size distribution index.

Note that the assumptions to derive Eq. 8 are: (1) fractal dimension D_f is less than 3; (2) P_c approaches infinity when S_{nw} = 1- S_{wr}. The two assumptions are also the constraints to use the Brooks-Corey capillary pressure model.

Eq. 8 foresees that the relationship between the capillary pressure and the normalized saturation of the wetting phase is linear on a log-log plot. This is true in many cases. However the accurate estimation of the residual wetting-phase saturation (S_{wr}) is important to obtain such a straight line from the capillary pressure data measured by a mercury intrusion approach. Overestimation and underestimation of the residual wetting-phase saturation may change the linear relationship on a log-log plot. This will be discussed later in more detail.

Experimental Measurements

Capillary pressure curves of different rock samples (Berea sandstone, chalk, and sandstone from an oil field) were measured using a mercury intrusion approach to obtain the fractal dimension.

The porosity of the Berea sandstone sample was about 23.0% and the air permeability was about 804 md. The Berea sandstone sample used in this study was the same as that used by Li and Horne[17]. The porosity of the chalk sample was about

29.3% and the air permeability was about 0.17 md. The porosity of the reservoir sandstone sample was about 27.1% and the air permeability was about 2131 md.

The surface tension of air/mercury is 480 mN/m and the contact angle through the mercury phase is 140^{o} according to the results reported by Purcell[21].

Results

Fractal dimension of porous media can be inferred from the capillary pressure curves using two methods (Eqs. 3 and 8) respectively. The values of fractal dimension calculated using Eq. 3 should be equal to those calculated using Eq. 8. To verify this, both theoretical and experimental capillary pressure curves were used in this study. The results are presented and analyzed in this section. Also discussed is the effect of the estimated residual wetting-phase saturation on the shape of the normalized capillary pressure curves.

Theoretical capillary pressure curves were calculated using different values of pore size distribution index, λ, to demonstrate the relationship between the fractal dimension and λ. Fig. 1 shows the capillary pressure curves calculated using the Brooks-Corey model (Eq. 8) with different values of λ. For simplicity, the residual wetting-phase saturation was fixed at 20% and the entry capillary pressure was fixed at 0.4 atm for all of the capillary pressure curves shown in Fig. 1. The values of λ ranged from 0.3 to 1.9. Fractal dimension can be inferred from the values of λ ($D_f = 3 - \lambda$).

The normalized wetting-phase saturations were calculated according to Eq. 9 and the relationships between capillary pressure and the normalized wetting-phase saturation were shown in Fig. 2. All of the relationships are straight lines as expected.

According to Eq. 3, the fractal dimension can be calculated once the relationship between capillary pressure and nonwetting-phase saturation gradient to the capillary pressure (dS_{nw}/dP_c) is known. The values of dS_{nw}/dP_c were calculated using the capillary pressure data shown in Fig. 1. The curves representing the relationship between dS_{nw}/dP_c and capillary pressure are shown in Fig. 3. All of the correlations are linear as foreseen in Eq. 3. The values of fractal dimension were calculated using Eq. 3 and were also inferred from the values of λ ($D_f = 3 - \lambda$). The results were compared and are listed in Table 1. One can see from Table 1 that the values of the fractal dimension inferred from the relationship between dS_{nw}/dP_c and capillary pressure (using Eq. 3) are very close to those calculated from the value of λ ($D_f = 3 - \lambda$).

To further demonstrate the relationship between the fractal dimension and the pore size distribution index, experimental capillary pressure curves were used. Fig. 4 shows the capillary pressure curves measured by using a mercury intrusion technique for different rock samples (Berea sandstone, chalk, and reservoir sandstone). The capillary pressure curves are different because the rock type and properties are different. Fig. 5 shows the corresponding normalized capillary pressure curves. Straight lines were obtained on a log-log plot. The values of the pore size distribution index were then calculated using Eq. 8 and the results are listed in Table 2. The values of fractal dimension were also determined from the values of λ ($D_f = 3 - \lambda$).

Fractal dimension can also be computed using the fractal model (Eq. 3) from the relationship between dS_{nw}/dP_c and capillary pressure. Fig. 6 shows the correlations between dS_{nw}/dP_c and capillary pressure of the three different rock samples. The values of the fractal dimension calculated using the data shown in Fig. 6 are listed in Table 2 and were compared with those inferred from the values of λ. One can see from Table 2 that the values of the fractal dimension calculated using the two methods are almost the same for the core samples studied.

The previous calculations based on both the theoretical and experimental capillary pressure curves demonstrate that the fractal dimension may be inferred directly using the Brooks-Corey capillary pressure model instead of using the relationship between dS_{nw}/dP_c and capillary pressure in many cases. One advantage to determine the fractal dimension from the Brooks-Corey capillary pressure model is that there is no need to calculate dS_{nw}/dP_c.

As mentioned previously, accuracy in estimating the residual wetting-phase saturation is essential to obtain the linear relationship between the capillary pressure and the normalized wetting-phase saturation. Fig. 7 shows the effect of overestimation and underestimation of the residual wetting-phase saturation on the normalized capillary pressure curves for λ=1.9. The true value of the residual wetting-phase saturation was 20% in Fig. 7. The values of the normalized wetting-phase saturation were calculated using Eq. 9 with different values of the residual wetting-phase saturation (see the numbers close to each curve in Fig. 7). One can see that the normalized capillary pressure curve is linear only when the estimated value of the residual wetting-phase saturation is equal to the true value (20%). The normalized capillary pressure curve is concave to the axis of the normalized wetting-phase saturation if the residual wetting-phase saturation is overestimated. Otherwise the normalized capillary pressure curve is convex to the axis of the normalized wetting-phase saturation. One can see from Fig. 7 that the effect of the residual wetting-phase saturation on the shape of the normalized capillary pressure curves is significant.

Fig. 8 also shows the effect of the estimated residual wetting-phase saturation on the shape of the normalized capillary pressure curves for λ=0.3. The phenomenon is similar to that shown in Fig. 7. However the effect of the estimated residual wetting-phase saturation on the normalized capillary pressure curves is more significant in the case with smaller value of λ than in the case with greater value of λ.

According to the results shown in Figs. 7 and 8, one can see that it is important to estimate the residual wetting-phase saturation accurately. Usually the true value of the residual wetting-phase saturation is smaller than the wetting-phase saturation at the maximum intrusion pressure during the mercury intrusion test. Brooks and Corey[1] used the “trial and error” technique to choose the residual wetting-phase saturation. In this study, the solver function of Microsoft Excel was used to estimate the residual wetting-phase saturation.

Note that if the normalized capillary pressure curve is concave to the axis of the normalized wetting-phase saturation, it does not always imply that the residual wetting-phase saturation is overestimated. For example, Li and Horne[17] found that the capillary pressure curves of the rock from The Geysers geothermal field are concave to the axis of the normalized wetting-phase saturation. This is not brought about by the overestimation of the residual wetting-phase saturation because the normalized capillary pressure curves are still concave to the axis of the normalized wetting-phase saturation even if the residual wetting-phase saturation is set to zero.

Discussion

Although a theoretical basis of the Brooks-Corey capillary pressure model has been found, it does not imply that the model can apply in all cases without constraints. As mentioned previously, there are two known constraints to use the Brooks-Corey capillary pressure model. One of the constraints is that P_c approaches infinity when S_{nw} = 1- S_{wr}. This may not be true in the case of imbibition capillary pressure curve. Sinnokrot[22] reported such an example. Sinnokrot[22] measured the oil-water capillary pressures of different rocks (limestones and sandstones) at different temperatures and found that the Brooks-Corey capillary pressure model could model the drainage oil-water capillary pressure curves but not the imbibition ones. For this reason, Li and Horne[23] proposed an empirical capillary pressure model for the imbibition case.

Another constraint to apply the Brooks-Corey capillary pressure model is that the fractal dimension D_f is less than 3 (less than 2 if the capillary tube model is used in the fractal modeling of the porous media). However the fractal dimension of the porous media with great heterogeneity may be greater than this value. For example, Li and Horne[17] found that the capillary pressure curves of the rock (with high density microfractures) from The Geysers geothermal field could not be represented using the Brooks-Corey capillary pressure model (although it could still be represented by a fractal model).

Conclusions

Based on the present work, the following conclusions may be drawn:

1. The Brooks-Corey capillary pressure model can be derived theoretically based on fractal modeling of porous media. This shows that the Brooks-Corey capillary pressure model, once considered as empirical, has a solid theoretical basis.
2. The pore size distribution index (λ) in the Brooks-Corey capillary pressure model increases with the decrease in fractal dimension (D_f) of the porous medium.
3. The fractal dimension of a porous medium may be inferred directly using the Brooks-Corey capillary pressure model instead of the fractal model in many cases.
4. Underestimation of the residual wetting-phase saturation may change the shape of the normalized capillary pressure curve from linear to nonlinear (convex to the axis of the normalized wetting-phase saturation) on a log-log plot.
5. Overestimation of the residual wetting-phase saturation may also change the shape of the normalized capillary pressure curve from linear to nonlinear (concave to the axis of the normalized wetting-phase saturation) on a log-log plot.

Acknowledgements

This research was conducted with financial support from the US Department of Energy under grant DE-FG07-02ID14418, the contribution of which is gratefully acknowledged.

Nomenclature

a = constant
b = constant
D_f = fractal dimension
P_c = capillary pressure
p_e = entry capillary pressure
S_{Hg} = mercury saturation
S_{nw} = nonwetting phase saturation
S_w = wetting phase saturation
S_w^* = normalized wetting-phase saturation
S_{wr} = residual saturation of the wetting phase
λ = pore size distribution index

References

1. Brooks, R.H. and Corey, A.T.: "Hydraulic Properties of Porous Media," Colorado State University, Hydro paper No.5 (1964).
2. Erkal, A. and Numbere, D.T.: "Relative Permeability Effets on the Migration of Steamflood Saturation Fronts," SPE 38299, presented at the 1997 SPE Western Regional Meeting, Long Beach, California, June 25-27, 1997.
3. Siddiqui, F. I.: "Defining Fluid Distribution and Fluid Contacts for Dynamically Charged Reservoirs," SPE 56513, presented at the 1999 SPE Annual Technical Conference and Exhibition held in Houston, Texas, October 3–6 1999.
4. Mikes, D., Barzandji, O.H.M., Bruining, J., and Geel, C.R.: "Upscaling of Flow Units for Reservoir Flow Incorporating Small-Scale Heterogeneities," SPE 68702, presented at the SPE Asia Pacific Oil and Gas Conference and Exhibition held in Jakarta, Indonesia, April 17–19 2001.
5. Kjosavik, A., Ringen, J.K., and Skjaeveland, S.M.: "Relative Permeability Correlation for Mixed-Wet Reservoirs," *SPEJ* (March 2002), 49-58.
6. Li, K. and Horne, R.N.: "Experimental Verification of Methods to Calculate Relative Permeability Using Capillary Pressure Data," SPE 76757, Proceedings of the 2002 SPE Western Region Meeting/AAPG Pacific Section Joint Meeting held in Anchorage, Alaska, May 20-22, 2002.
7. Papatzacos, P. and Skjæveland, S.M.: "Relative Permeability from Capillary Pressure," SPE 77540, presented at the 2002 SPE Annual Technical Conference and Exhibition, San Antonio, TX, USA, September 29 to October 02, 2002.
8. Katz, A.J. and Thompson, A.H.: "Fractal Sandstone Pores: Implications for Conductivity and Pore Formation," *Phys. Rev. Lett.*, **54**, 1325-1328 (1985).

9. Friesen, W.I. and Mikula, R.J.: "Fractal Dimensions of Coal Particles", *J. of Colloid and Interface Science*, **120**(1), 263-271 (November 1987).
10. Hansen, J.P. and Skjeltorp, A.T.: "Fractal Pore Space and Rock Permeability Implications," *Phys. Rev.* B, **38**(4), 2635-2638 (1988).
11. Krohn, C.E.: "Fractal Measurements of Sandstones, Shales, and Carbonates," *J. of Geophysical Research*, **93**(B4), 3297-3305 (1988).
12. Lenormand, R.: "Gravity-Assisted Inert Gas Injection: Micromodel Experiments and Model Based on Fractal Roughness," The European Oil and Gas Conference, Altavilla Milica, Palermo, Sicily, October 9-12, 1990.
13. Angulo, R.F. and Gonzalez, H.: "Fractal Dimensions from Mercury Intrusion Capillary Tests," SPE 23695, presented at the 2nd Latin American Petroleum Engineering Conf. of SPE held in Caracas, Venezuela, March 8-11, 1992.
14. Toledo, P.G., Novy, R.A., Davis, H.T., and Scriven, L.E.: "Capillary Pressure, Water Relative Permeability, Electrical Conductivity and Capillary Dispersion Coefficient of Fractal Porous Media at Low Wetting Phase Saturations" *SPE Advanced Technology Series* (1993), **2**(1), 136-141.
15. Shen, P. and Li, K.: "A New Method for Determining the Fractal Dimension of Pore Structures and Its Application," Proceedings of the 10th Offshore South East Asia Conference, Singapore, December 6-9, 1994.
16. Shen, P. and Li, K.: "Quantitative Description for the Heterogeneity of Pore Structure by Using Mercury Capillary Pressure Curves," SPE 29996, Proceedings of the SPE International Meeting held in Beijing, China, November 14-17, 1995.
17. Li, K. and Horne, R.N.: "Fractal Characterization of The Geysers Rock," presented at the Geothermal Resource Council 2003 annual meeting, October 12-15, 2003, Morelia, Mexico; GRC *Trans*. **27** (2003).
18. Li, K.: "Characterization of Rock Heterogeneity Using Fractal Geometry," SPE 86975, Proceedings of the 2004 SPE Western Region Meeting, Bakersfield, CA, USA, March 16-18, 2004.
19. Abdassah, D., Permadi, P., and Sumantri, R.: "Saturation Exponents Derived from Fractal Modeling of Thin Sections," SPE 36978, presented at the 1996 SPE Asia Pacific Oil and Gas Conference held in Adelaide, Australia, October 28-31-17, 1996.
20. Moulu, J-C., Vizika, O., Kalaydjian, F., and Duquerroix, J-P.: "A New Model for Three-Phase Relative Permeabilities Based on a Fractal Representation of the Porous Media," SPE 38891, presented at the SPE Annual Technical Conference and Exhibition, San Antonio, TX, USA, October 5-8, 1997.
21. Purcell, W.R.: "Capillary Pressures-Their Measurement Using Mercury and the Calculation of Permeability", *Trans. AIME*, (1949), **186**, 39.
22. Sinnokrot, A.A: The Effect of Temperature on Oil-Water Capillary Pressure Curves of Limestones and Sandstones, Ph.D. dissertation, Stanford University, Stanford, CA, USA (1969).
23. Li, K. and Horne, R.N.: "An Experimental and Theoretical Study of Steam-Water Capillary Pressure," *SPEREE* (December 2001), p.477-482.

Table 1: Fractal dimension calculated using different methods.

λ		0.3	0.5	0.7	1.1	1.9
D_f	3-λ	2.7	2.5	2.3	1.9	1.1
	Eq. 3	2.73	2.53	2.33	1.94	1.16

Table 2: Fractal dimension and pore size distribution index calculated for different rock samples.

rock		Berea	Chalk	Reservoir rock
λ		0.674	1.572	0.542
D_f	3-λ	2.326	1.428	2.458
	Eq. 3	2.451	1.494	2.471

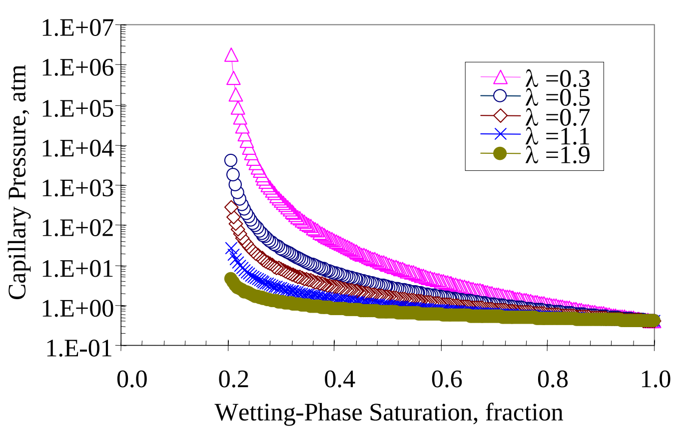

Fig. 1: Capillary pressure curves with different values of pore size distribution index.

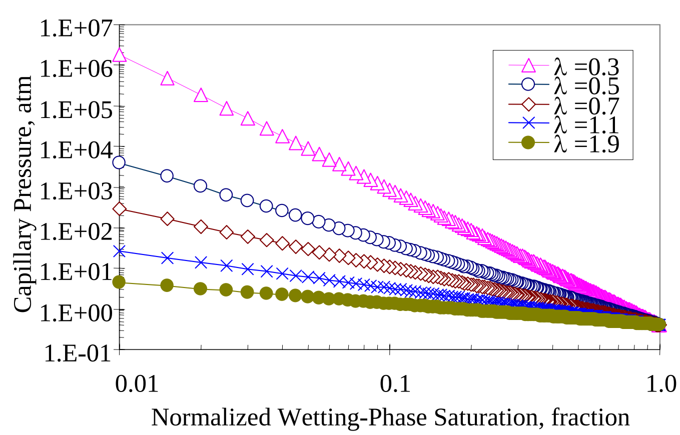

Fig. 2: Normalized theoretical capillary pressure curves with different values of pore size distribution index.

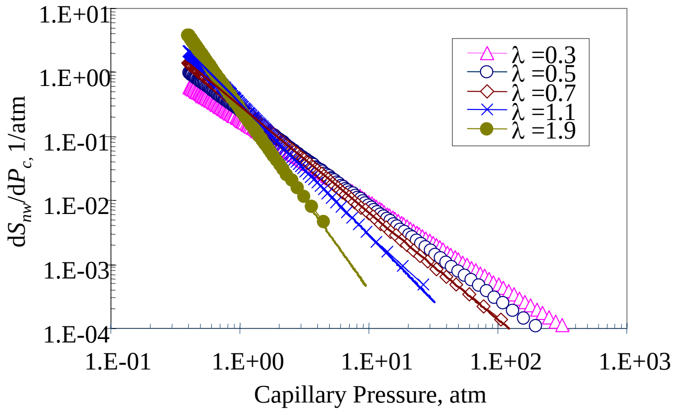

Fig. 3: Relationship between dS_{nw}/dP_c and capillary pressure for different values of pore size distribution index.

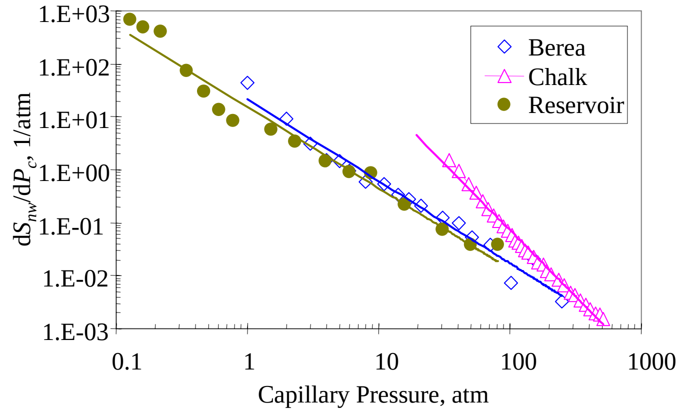

Fig. 6: Relationship between dS_{nw}/dP_c and capillary pressure for different rocks.

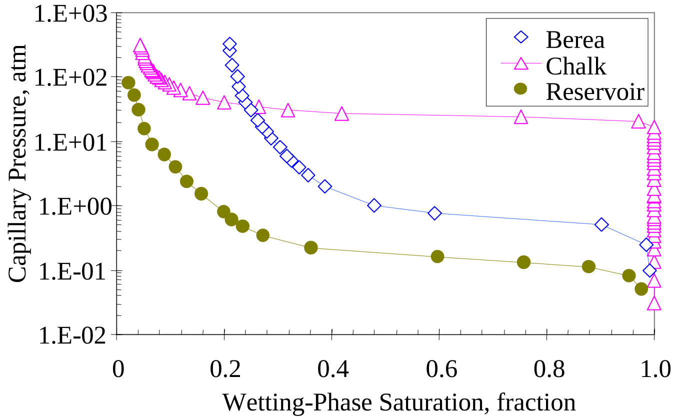

Fig. 4: Capillary pressure curves of different rocks (Berea sandstone, chalk, and reservoir rock).

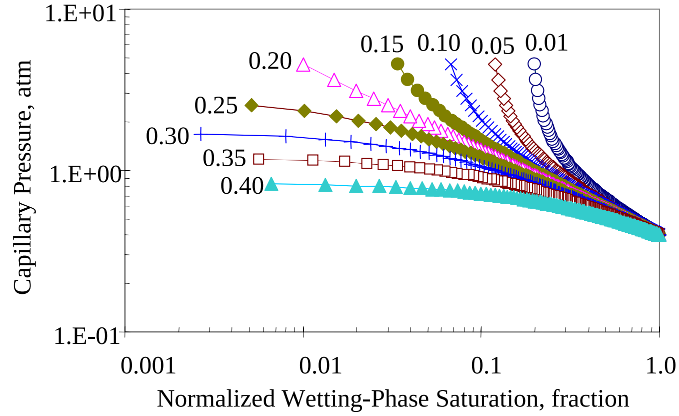

Fig. 7: Effect of residual wetting-phase saturation on the estimation of normalized capillary pressure curves (λ=1.9).

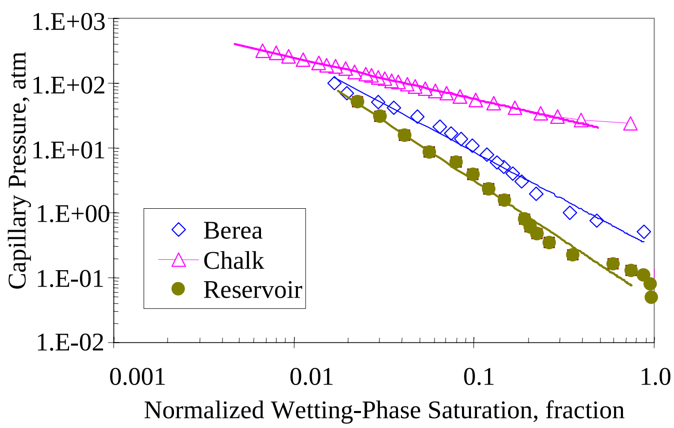

Fig. 5: Normalized capillary pressure curves of different rocks (Berea sandstone, chalk, and reservoir rock).

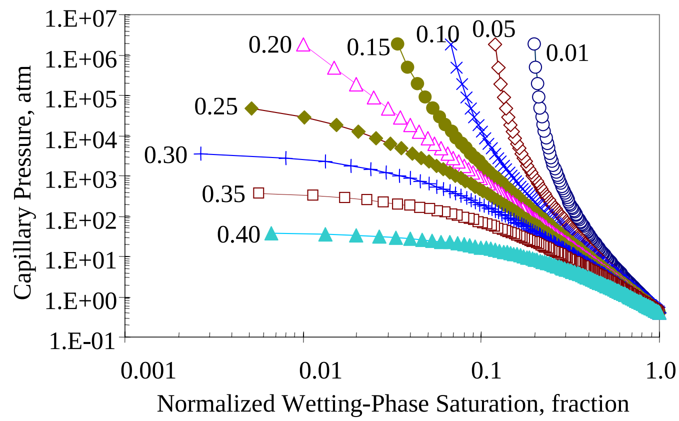

Fig. 8: Effect of residual wetting-phase saturation on the estimation of normalized capillary pressure curves (λ=0.3).